

Using functional magnetic resonance imaging to explore the flashed face distortion effect

Tanya Wen

Department of Psychology, National Cheng Kung University, Tainan City, Taiwan

Department of Life Sciences, National Cheng Kung University, Tainan City, Taiwan



Chun-Chia Kung

Department of Psychology, National Cheng Kung University, Tainan City, Taiwan



The flashed face distortion (FFD) effect was coined by Tangen, Murphy, and Thompson (2011) in their second-place winner of the 2012 Best Illusion of the Year Contest. The FFD arises when people view various eye-aligned faces that are sequentially flashed in the visual periphery, and gradually the faces appear to be deformed and grotesque. In this functional magnetic resonance imaging (fMRI) study, participants were presented with four conditions: (a) one face pair changing only its illumination; (b) two and (c) three alternating face pairs; and (d) nonrepeated face pairs. Participants rated the magnitude of each illusion immediately after each block. Results showed that the receptive region of the early visual cortex (V1–V4), and category-selective areas such as the fusiform face area (FFA) and occipital face area (OFA), responded proportionally to the participants' rated FFD strength. A random-effects voxelwise analysis further revealed positively correlated areas (including the medial and superolateral frontal areas) and negatively correlated areas (including the precuneus, postcentral gyrus, right insula, and bilateral middle frontal gyri) with respect to participants' ratings. Time series correlations among these nine ROIs (four positive and five negative) indicated that most participants showed a clustering of the two separate ROI types. Exploratory factor analysis (EFA) also demonstrated the segregation of the positive and negative ROIs; additionally, two subsystems were identified within the negative ROIs. These results suggest that the FFD is mediated by at least two networks: one that is likely responsible for perception and another that is likely responsible for subjective feelings and engagement.

Introduction

Illusions are misinterpretations of true stimuli or distortions of the outside world resulting from brain mechanisms that work extraordinarily well most of the time (Gregory, 1968). Visual processing usually chooses the most efficient, rather than the most accurate, routes (i.e., heuristics), thereby producing illusions. Therefore, illusions are more related to the brain's interpretation of the external sensory input than to the stimuli per se (Eysel, 2003).

A number of neuroimaging studies have shown that neural activities in sensory areas are involved in the illusions. Examples include a portion of the color-selective area in the ventral occipital cortex found to be activated when participants perceive illusory color (Morita et al., 2004); the hMT+ activated in the Rotating Snakes illusion despite its stationary display in reality (Kuriki, Ashida, Murakami, & Kitaoka, 2008); and the comparative stronger FFA activities when participants perceive faces (vs. vases) in the Rubin's vase–face illusion (Andrews, Schluppeck, Homfray, Matthews, & Blakemore, 2002; Hasson, Hendler, Ben Bashat, & Malach, 2001). These studies illustrate the usefulness of neuroimaging in unraveling the neural underpinnings of various illusions.

Similar to the above-mentioned studies, the present research aims to investigate the neural correlates of the flashed face distortion (FFD; Tangen, Murphy, & Thompson, 2011). The FFD is commonly illustrated by presenting a series of eye-aligned faces, at an optimal frequency of 2–4 Hz, in the visual periphery. After fixating on the central cross while faces are presented bilaterally, people gradually perceive that facial fea-

Citation: Wen, T., & Kung, C.-C. (2014). Using functional magnetic resonance imaging to explore the flashed face distortion effect. *Journal of Vision*, 14(12):29, 1–13, <http://www.journalofvision.org/content/14/12/29>, doi:10.1167/14.12.29.

tures (such as eyes and mouths) become distorted and occasionally even bizarre or grotesque.

Despite the FFD's overwhelming popularity, there seems to be no follow-up work after the initial publication by Tangen et al. (2011), who suggested that relative encoding, i.e., encoding each face in comparison to others in the visual periphery, may play a role in the disproportionate magnification of featural differences. Echoing the observation above, our prior series of experiments (Wen & Kung, 2012) found that the perceived FFD strength was compromised when the number of faces was small.

Given the behavioral findings we have noted, in this fMRI study, we manipulated the number of faces in different blocks (1, 2, 3, or 64) to vary the perceived FFD strength. Early and intermediate visual areas (from the primary visual cortex to face-selective areas) were functionally defined as regions of interest. Additional brain regions that were significantly correlated with the perceived FFD strength were identified by voxelwise multiple regression. Lastly, functional connectivity using exploratory factor analysis was carried out to further categorize these brain regions subserving the FFD. We hypothesize that, because the FFD involves perceptual and emotional components, separable neural networks corresponding to these aspects could be characterized.

Methods

Participants

Fourteen healthy participants (eight male and six female) with normal or corrected-to-normal vision participated in the experiment (age range = 20–33 years, $M = 23.36$, $SD = 3.16$). The participants gave informed consent before the study began and were paid 500 NTD after completion.

Stimuli and procedure

A set of 100 eye-aligned Slovakian faces obtained from the supplementary online materials (<http://dx.doi.org/10.1068/p6968>) provided by Tangen et al. (2011) were used in this experiment. Stimuli presentation was rear-projected onto a screen inside the MRI scanner that was situated 95 cm from the observer. Participants viewed the display through a mirror that was placed above the head coil. Two series of sequential face images (7.5 cm × 5 cm) were presented peripherally, 3° to each side of the fixation point to produce the FFD illusion. Participants were asked to keep their eyes fixated on the cross during the presentation to achieve

the optimal effect. Stimulus presentation was controlled in Matlab (2009a, The MathWorks, Inc., Natick, MA) using Psychtoolbox (Brainard, 1997).

The experiment consisted of four types of blocks: control (CON), 2-Face-Repeat (2FR), 3-Face-Repeat (3FR), and No-Repeated-Faces (NRF). Each quad of blocks was presented a total of eight times across four runs. In the CON condition, the pair of faces was fixed and changed only in its illumination. In the 2FR condition, two alternating pairs of faces were presented. In the 3FR condition, a sequence of three face pairs cycled repeatedly. Finally, the NRF condition consisted of a sequence of nonrepeated face pairs, where each face pair appeared just once (see Figure 1). In all four block types, each illumination or face was shown for 250 ms before being consecutively followed by the next illumination or face. The order of each block was pseudorandomized; the faces were randomly chosen for each block and programmed not to overlap in the CON, 2FR, and 3FR conditions. The duration of each block was 16 s, followed by the administration of a 4-point scale that lasted up to 4 s until the participant completed rating the degree of perceived deformation of the faces (with 1 indicating the weakest and 4 indicating the strongest face deformation) by pressing a button on a response pad. Afterwards, a 12-s interblock fixation/rest period preceded the next block.

ROI localizing experiments

Functional localization of face-responsive areas

Pictures of bodies, Caucasian faces, scenes, and cars were presented within the blocks to the participants. Each block contained 20 images of the same category, centered at the fixation; each stimulus was displayed for 350 ms, followed by a 350-ms interstimulus interval, for a total of 14 s per block. During the presentation, participants performed a one-back task by pressing the trigger when a stimulus was spotted appearing twice in a row. A 14-s fixation was interleaved every four blocks. Each block type was repeated four times for two runs (therefore eight times in total).

To define face-responsive ROIs, a single subject general linear model (GLM) was applied, with the contrast of faces versus scenes, thresholded at the false discovery rate (FDR) of $q < 0.05$ to correct for multiple comparisons. Three common face-responsive areas were delineated for each participant, including the fusiform face area (FFA), the occipital face area (OFA), and the superior temporal sulcus (STS). As facial processing is dominated by the right hemisphere (Haxby, Hoffman, & Gobbini, 2000), the subsequent analyses exclusively focused on the right FFA, OFA, and STS.

The rFFA was identified in all 14 participants, with average Talairach coordinates ($\pm SE$) of 36.47(1.1),

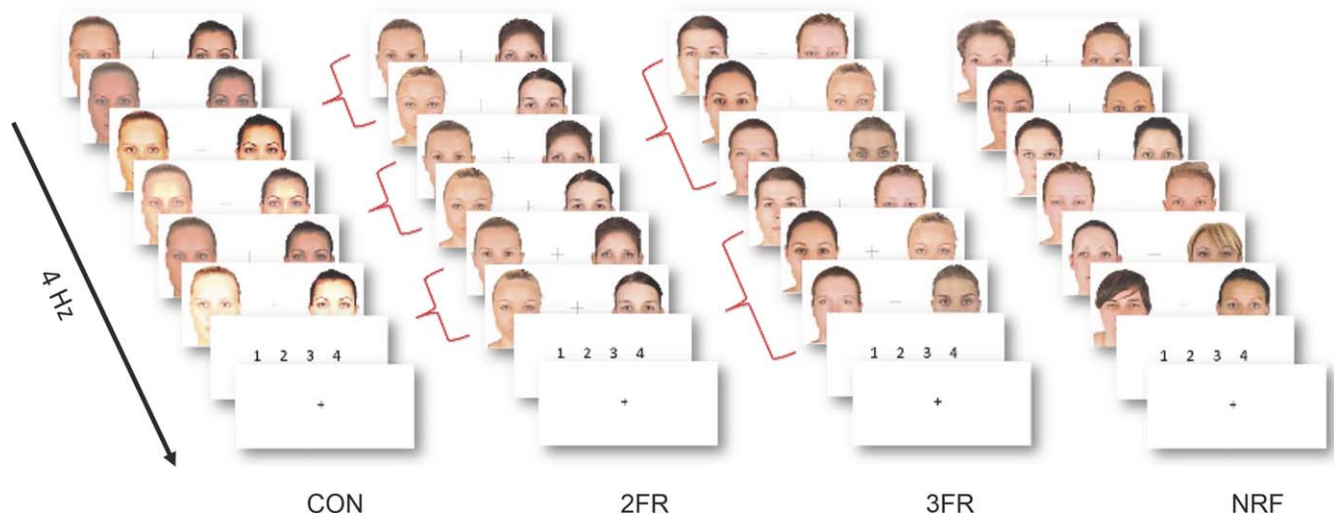


Figure 1. The block design presentation of the FFD experiment. Participants viewed blocks (16 s each) of face sequences with different numbers of repeated faces (one, two, three, or nonrepeated; repetitions are shown with brackets above) and were asked to rate the magnitude of the illusion at the end of each block (up to 4 s).

−47.94(1.34), and −15.6(1.42); the rOFA was identified in all 14 participants, with average Talairach coordinates ($\pm SE$) of 37.43(1.11), −72.91(1.26), and −8.25(1.08); and the rSTS was identified in 12 of the 14 participants, with average Talairach coordinates ($\pm SE$) of 44.24(1.26), −40.67(1.76), and 11.52(1.74). The results are shown in Figure 2a.

Retinotopic mapping of early visual areas

To define the retinotopic visual areas, a flickering checkerboard (4 Hz) superimposed onto a rotating bowtie (45° each side) was used. The rotating bowtie completed a full cycle every 32 s and each run included eight cycles. While fixating on the center of the screen, participants were given a fixation-dimming detection task to help maintain their focus on the stimuli. At the center of the screen, the fixation dimmed at random times throughout the run and participants were asked to press a button if dimming was detected. Each participant completed five or six runs.

Retinotopic maps for each participant were obtained by performing cross correlation analyses, followed by the delineation of areas V1v/d, V2v/d, V3v/d, and V4v/d. Activation maps of the FFD conditions were individually created by contrasting areas that responded more strongly to the FFD blocks than fixation (with $q < 0.05$ as the threshold). This map was then overlapped with the retinotopic maps of each participant to circumvent the FFD task-related areas in the early visual cortex. These early visual ROIs spread over V1–V4 (Wandell & Smirnakis, 2009; Warnking et al., 2002).

Visual areas V1v/d, V2v/d, V3v/d, and V4v/d were delineated in each participant and overlapped with

FFD task-driven activation (see Figure 2b). In one subject, we could not delineate V4d in the left hemisphere.

Imaging parameters and data analysis

Imaging was performed using the GE MR750 3T scanner (GE Medical Systems, Waukesha, WI) located in the MRI center of National Cheng Kung University. High resolution anatomical images were acquired using fast spoiled gradient echo (fast-SPGR), consisting of 166 axial slices (TR = 7.6 ms, TE = 3.3 ms, flip angle = 12°, 224 × 224 matrices, slice thickness = 1 mm). Functional images were acquired using a gradient-echo echo-planar imaging (EPI) pulse sequence (TR = 2000 ms, TE = 33 ms, flip angle = 76°, 64 × 64 matrices, slice thickness = 3 mm, no gap, voxel size 3 × 3 × 3 mm³, 40 axial slices covering the entire brain).

Data were preprocessed and analyzed using BrainVoyager QX (Brain Innovation, Maastricht, The Netherlands). Functional images were corrected for head movements using six-parameter rigid transformations, after slice timing correction, by realigning all volumes to the first functional volume. Neither high-pass filtering nor spatial smoothing was applied. For each participant, the functional scan was coregistered to the anatomical scan and then transformed into Talairach space (Talairach & Tournoux, 1988). ROI analyses for face-responsive areas were applied in this volume space. For retinotopic mapping, the anatomical volume for each subject was inflated, cut along the calcarine sulcus, and flattened into a surface map.

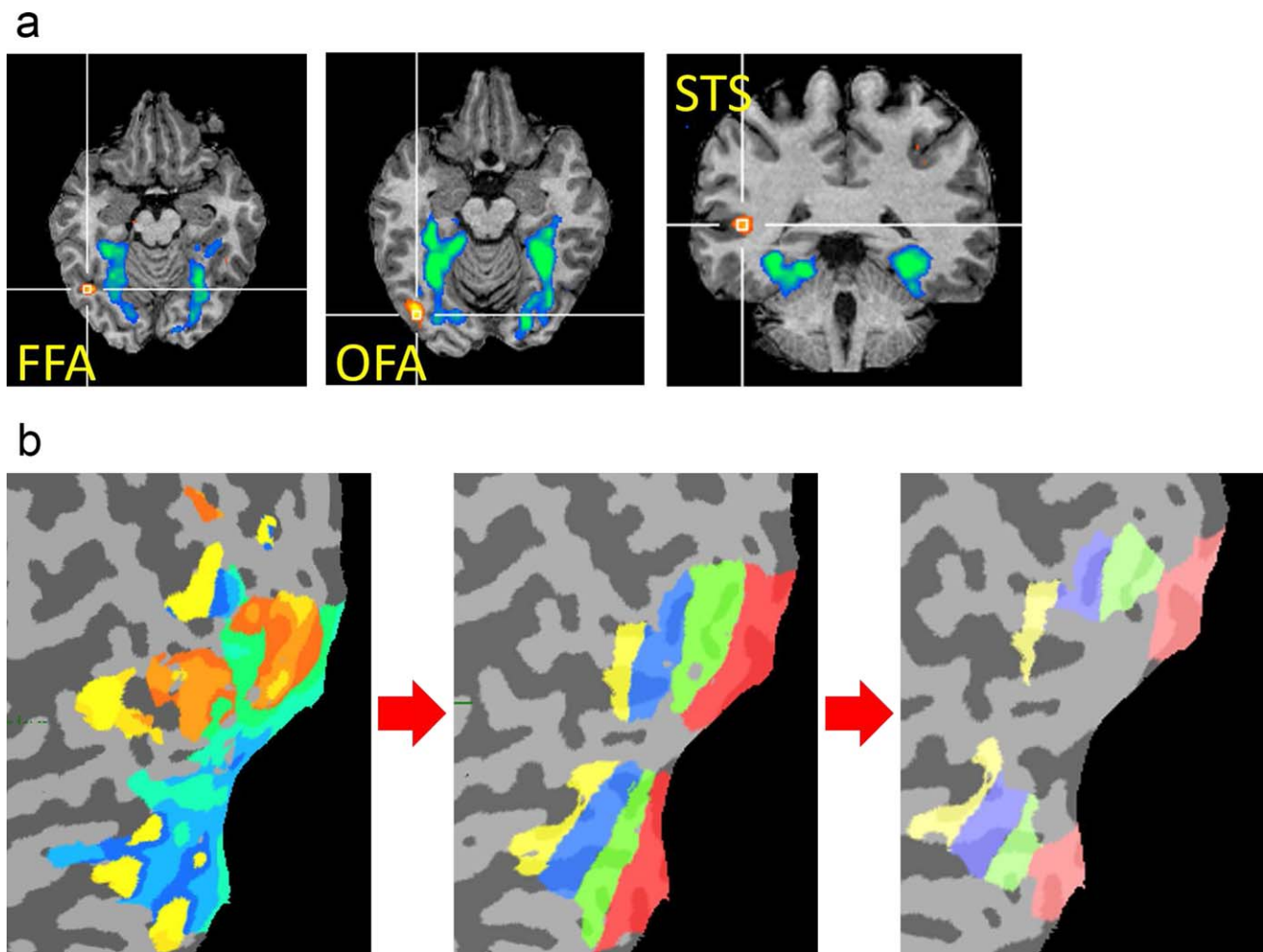


Figure 2. (a) The face-selective areas defined by the localizer task. (b) The early visual areas were demarcated (V1–V4) and then overlapped with FFD task-driven activation.

Time course analysis and ROIs

To obtain the BOLD responses for each condition in the FFD experiment, event-related averaging was performed within each participant's ROIs. The BOLD signal responses were then averaged across the stimulation presentation period (3–10 time points with respect to the onset of the FFD display to account for hemodynamic response delay) for each block type. The data from early visual areas were averaged across the two hemispheres. The four FFD conditions (CON, 2FR, 3FR, NRF) were analyzed using a one-way repeated-measure ANOVA, and the post hoc *t* tests assessed how activations differed among these conditions.

To link the brain activities and subjective perceptual FFD strength, a multiple regression analysis was performed using the average ratings from the four conditions as predictors and a dummy variable for each subject (as done in Morita et al., 2004). Thus, each subject provided four data points in the analysis. First,

this was performed within each predefined ROI, then in the entire brain (i.e., a random-effects voxelwise correlation) to identify voxels that showed activities correlated with the perceptual FFD strength. The regression coefficient was thresholded at $p < 0.05$, and a minimum contiguity of 30 voxels, as a cluster.

Functional connectivity

After identifying additional ROIs using the random-effects voxelwise correlation analysis, we further examined their coherence of averaged time courses with one another. To this end, exploratory factor analysis (EFA) is a useful way to simultaneously categorize distinct neural systems, i.e., regions that function in accordance during a particular task. When a brain region belongs to a particular factor, it is assumed to have similar roles with other regions that belong to the same functional network (Koshino et al., 2005; Mashal, Faust, & Hendler, 2005; McLaughlin et al., 1992;

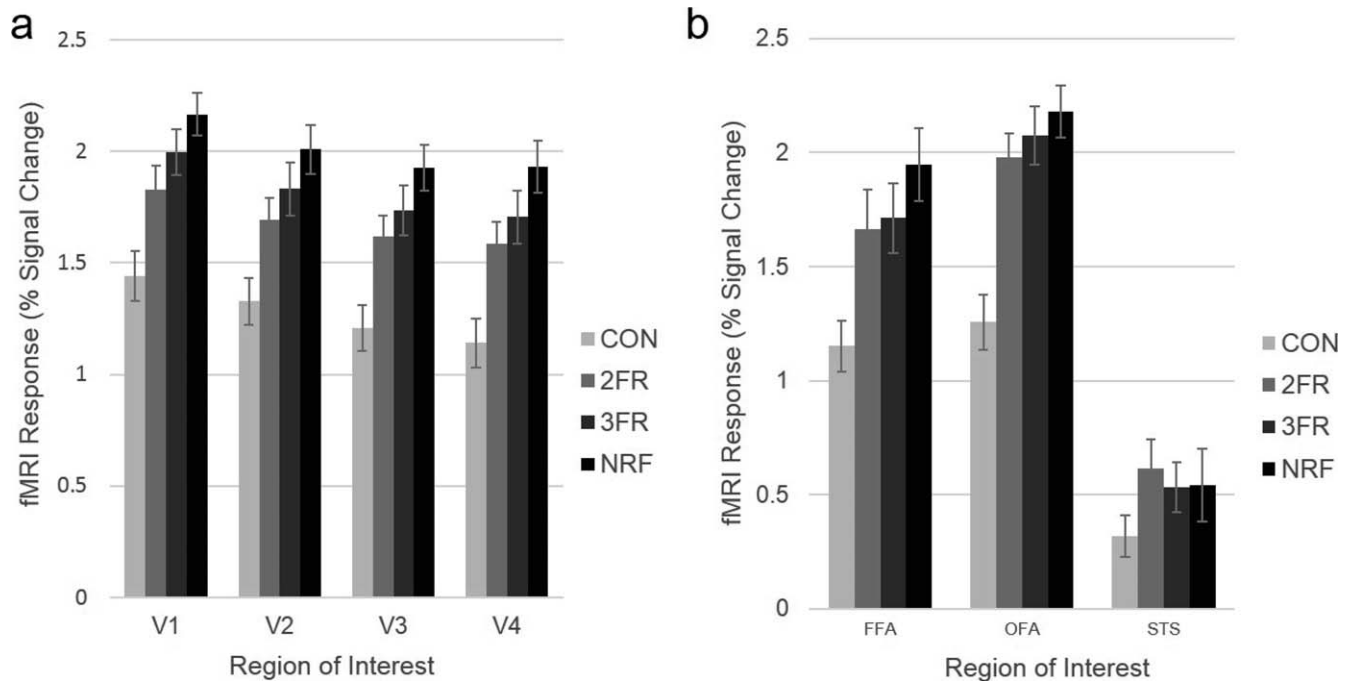


Figure 3. Percent signal change in each ROI across the four types of presentations in (a) the early visual areas and (b) face-selective areas. Error bars indicate ± 1 SEM.

Peterson et al., 1999). To perform EFA, the scans of the four runs were concatenated, and time series correlations were performed across the nine chosen ROIs. This process was performed for every individual, and then the data were averaged across all participants, resulting in a 532 (volumes) \times 9 (ROIs) matrix. The correlation matrix was then decomposed, and the factors underwent varimax rotation to separate the ROIs into higher order structures; this analysis also served as a cross-

validation of the aggregated brain networks, indicating either a positive or negative correlation with the subjects' subjective ratings.

Results

ROI analysis

In each ROI (rFFA, rOFA, rSTS, V1-ffd, V2-ffd, V3-ffd, and V4-ffd), a repeated measures one-way ANOVA was performed to compare the BOLD responses across each of the four conditions (CON, 2FR, 3FR, NRF). The graphs of average percent signal changes are shown in Figure 3. The four experimental conditions produced a significant effect in six of the ROIs, all $F_s(1, 13) > 50.11$, $p_s < 0.001$ in rFFA, rOFA, V1-ffd, V2-ffd, V3-ffd, and V4-ffd; however, a significant effect was not observed in the rSTS, $F(1,11) = 4.06$, $p = 0.07$. Post hoc comparisons with Bonferroni corrections (over six joint pairwise comparisons for the six ROIs) showed that a trend of $NRF > 3FR > 2FR > CON$ was observed in each of the six ROIs described above (detailed analysis shown in Supplementary Table S1).

Evaluation of the manipulation of FFD strength was confirmed by calculating a high correlation between the average participant rating and the experimental condition; ratings gradually increased as the number of faces increased ($r = 0.989$, $p < 0.001$, Figure 4). Interrater reliability (Cronbach's $\alpha = 0.996$) was high.

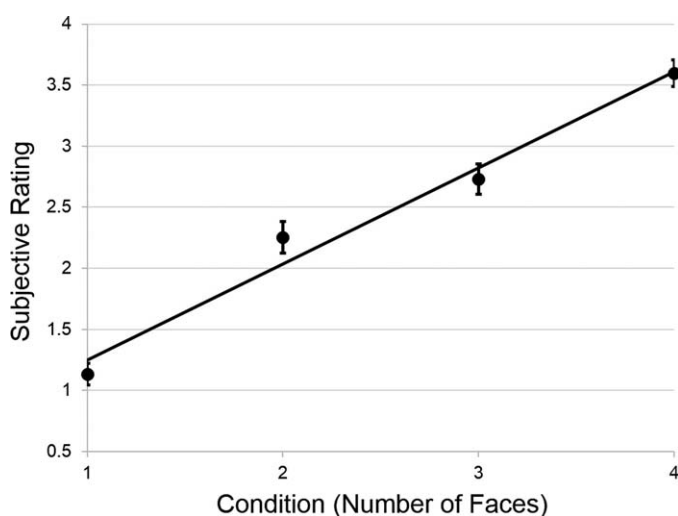


Figure 4. The average rating of the FFD strength elicited by the number of faces in each condition (CON, 2FR, 3FR, and NRF) in all 14 participants ($r = 0.989$, $p < 0.001$). Error bars depict ± 1 SEM.

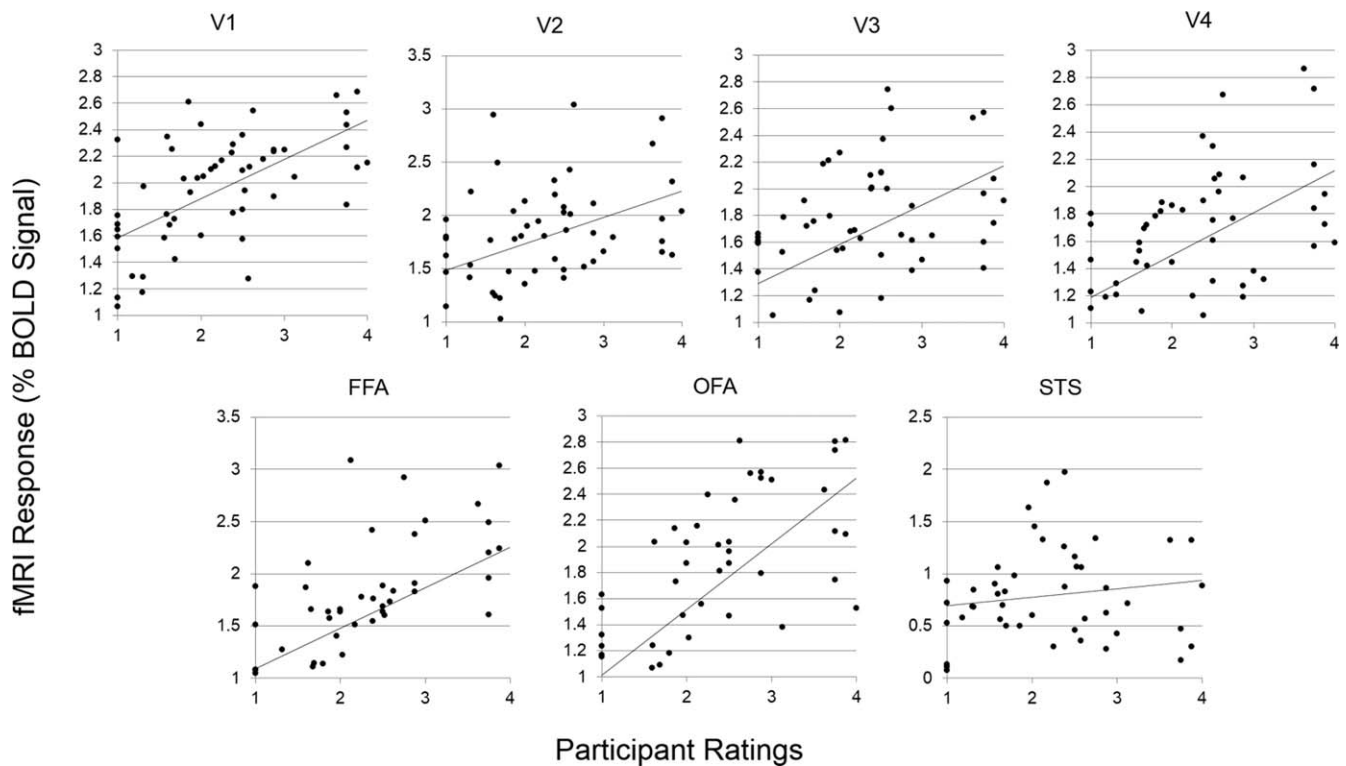


Figure 5. Percent signal change correlated with subjective illusion magnitude. The scatterplots show the relationship between the BOLD response in the visual ROIs for each rating scale.

To account for subjective perception and stochastic variability in illusion strength, our multiple linear regression analysis examined the relationship between BOLD activity in the ROIs and participants' FFD rating. In all ROIs, the regression coefficients for participants' ratings were all significantly greater than zero—all $t_s(41) > 8.72$, $p_s < 0.001$ in rFFA, rOFA, V1-ffd, V2-ffd, V3-ffd, and V4-ffd; $t(35) = 3.03$, $p = 0.005$ in rSTS—indicating a positive correlation between subjective perceptual strength and PSC, as shown in Figure 5.

Thus, each participant provided four data points. A multiple regression analysis of participant ratings and BOLD response in each ROI, with a dummy variable for each participant, showed linear trends that were significant in all seven ROIs. All $t_s(41) > 8.72$, $p_s < 0.001$ in rFFA, rOFA, V1-ffd, V2-ffd, V3-ffd, and V4-ffd; $t(35) = 3.03$, $p = 0.005$ in rSTS.

Random-effects voxelwise analysis

To identify all brain regions that showed activity in accordance with subjective FFD strength, a random-effects voxelwise correlation analysis was performed for all brain voxels. As expected, there was a huge patch of the extrastriate cortex, extending to engulf the OFA and FFA, significantly correlated with subjects' ratings.

In addition to these visual areas, other parieto-temporal-frontal areas, including the precuneus, bilateral middle frontal gyrus, right insula, postcentral gyrus, and left superior temporal sulcus, all negatively correlated with the FFD strength, and both the bilateral medial, inferior, and superior frontal gyri positively correlated with perceptual FFD strength (see Table 1, Figures 5 and 6).

ROI time course correlations

Pearson's correlation coefficients for the concatenated time courses (collapsing the four FFD runs) between the identified ROIs were calculated. The values of the correlation coefficients ranged from 0.25 and 0.81. The lowest correlation was between the right inferior frontal and left middle frontal gyri; the highest correlation was between the left and right inferior frontal gyri. The average correlation coefficient across all of the selected ROIs was 0.46.

As the ROIs can be divided into those that were positively and negatively correlated with BOLD activity, it would be worthwhile to compare these ROIs separately. The average coefficient for the positively correlated ROIs (i.e., visual areas, bilateral medial and superolateral frontal areas) was 0.73; the average coefficient for the negatively correlated ROIs (i.e.,

Region	L/R/B	±	Talairach			Cluster size	CON		2FR		3FR		NRF	
			x	y	z		Voxels	t values	p values	t values	p values	t values	p values	t values
Visual-parietal areas	B	+	2	-71.38	1.59	120,237	14.68	<0.0001	32.537	<0.0001	33.414	<0.0001	40.873	<0.0001
Medial frontal gyrus	B	+	-3.18	5.71	50.32	3564	-0.681	0.496	12.286	<0.0001	9.316	<0.0001	10.863	<0.0001
Superolateral frontal areas	R	+	37.37	4.1	35.95	9745	10.831	<0.0001	27.001	<0.0001	22.477	<0.0001	26.332	<0.0001
	L	+	-42.96	-4.75	37.42	5369	4.023	<0.0001	17.187	<0.0001	12.334	<0.0001	16.985	<0.0001
Precuneus-postcentral gyrus	B-L	-	3.08	-45.61	44.95	11,274	-10.48	<0.0001	-16.687	<0.0001	-19.159	<0.0001	-19.816	<0.0001
Insula	R	-	38.09	-10.86	11.52	1381	-3.694	<0.0001	-6.101	<0.0001	-11.892	<0.0001	-11.268	<0.0001
Middle frontal gyrus	R	-	32.99	36.08	34.98	1200	-3.676	<0.0001	-4.809	<0.0001	-7.628	<0.0001	-8.354	<0.0001
	L	-	-33.99	33.83	37.49	1495	-4.044	<0.0001	-10.085	<0.0001	-13.7	<0.0001	-10.672	<0.0001
Superior temporal gyrus	L	-	-59.78	-30.06	20.85	8887	-7.265	<0.0001	-10.637	<0.0001	-15.464	<0.0001	-17.857	<0.0001

Table 1. Regions that were significantly correlated with subjective ratings of FFD strength. Note: L/R/B stands for left, right, and bilateral.

precuneus-postcentral gyrus, right insula, bilateral middle frontal gyri, and left superior temporal sulcus) was 0.5 (the difference, $t(12) = 3.72, p = 0.002$). In contrast, the average the time series correlation between positively and negatively rating-correlated ROIs was 0.36 (see Figure 8b). These regions showed significant differences between same and different directions of correlation, $t(32) = 5.35, p < 0.001$.

Exploratory factor analysis

We subsequently performed an exploratory factor analysis on the ROI data to further elucidate their internal structure, to further explore the relationship within and between positively and negatively rating-correlated ROIs. Typically, the outcomes of exploratory factor analysis would show their clustering between ROIs of similar time series.

As shown by the factor loadings in Table 2, decomposition of the correlation matrix suggested the extraction of three factors. The first factor consisted of the four positive rating-correlated ROIs (visual areas, medial frontal gyrus, and bilateral superolateral frontal areas). The second factor was dominated by the precuneus-postcentral gyrus, the right insula, and the left superior temporal sulcus. The last factor was the left and right middle frontal gyri pair. Therefore, not only can these nine ROIs be divided into positively and negatively correlated subgroups, the negative group can be further separated into two subsystems. To verify the results above and compare the effect of different inputs on the EFA outcome, the same procedure was performed on the concatenated time courses corresponding to each condition. Similar results were obtained and shown in the supplementary materials.

Discussion

The present study aims to investigate the neural substrates of the FFD effect. By manipulating the strength of the illusion with the number of faces presented per cycle, we found that the BOLD responses in the retinotopy-defined early visual areas and the localizer-defined face-selective areas (rFFA, rOFA, and rSTS) both showed corresponding changes (Figure 3), which correlated with the subjects' ratings (Figure 5). In addition, voxelwise correlations revealed not only the above-mentioned visual areas (corroborating with the results from ROI analysis approach), but also frontal, temporal, and parietal rating-correlated regions (Figure 6). The average time course of these nine ROIs (Figure 7) can be visually categorized into two groups: one convex (outlined in red) and one concave

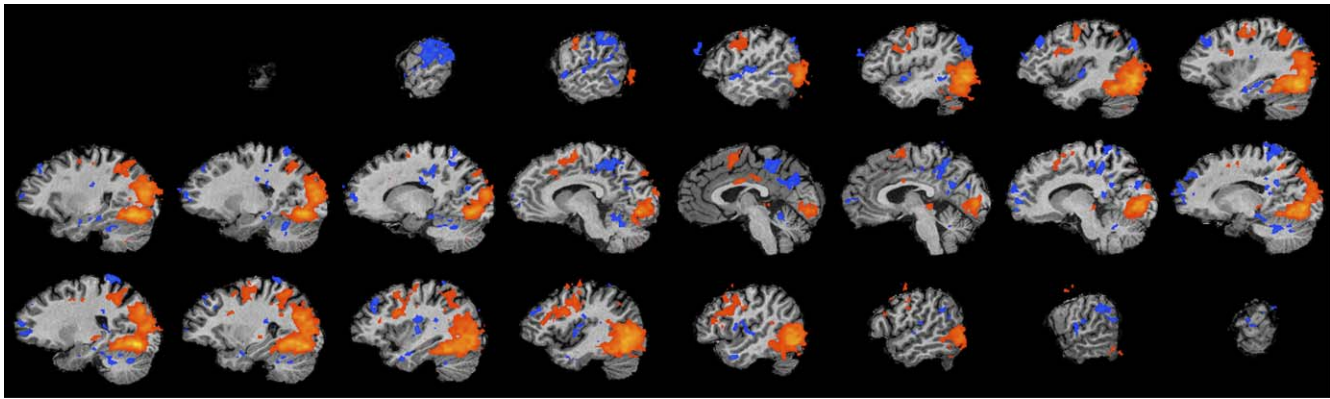


Figure 6. Montage visualization of the brain regions that were correlated with the participants' ratings.

(outlined in blue) in shape. To further examine the relationship among these nine ROIs, a time series correlation matrix was constructed (Figure 8a). Regions that were positively correlated with ratings showed higher intracorrelations (0.73) than those regions that were negatively correlated with ratings (0.5); and both were larger than the intercorrelation (0.36) between these two groups. Finally, an exploratory factor analysis independently verified the separation of positively and negatively correlated areas and determined that the negative areas could be further divided into two subsystems (Table 2).

The aforementioned systems that were positively and negatively correlated with ratings are most likely jointly tuned to the perception- and appraisal-related processing of the FFD. Among the positively correlated regions, the visual-parietal areas have been associated with perception- (de Borst et al., 2012; Woolgar, Thompson, Bor, & Duncan, 2011), action- (Corina et al., 2007), and attention-related (Roth, Johnson, Raye, & Constable, 2009) processing of stimuli. The medial frontal region is related to motor (Baumann et al., 2007) and attentional (Habeck et al., 2005) processing, and is also a component of the default mode network (Wang et al., 2007). The bilateral superolateral areas have been associated with the integration of emotion

ROI	Factor loadings		
	1	2	3
(1) Visual-parietal areas	0.78	0.13	0.15
(2) Medial frontal gyrus	0.72	0.36	0.15
(3) Right superolateral frontal gyrus	0.90	0.21	0.13
(4) Left superolateral frontal gyrus	0.81	0.38	0.10
(5) Precuneus-postcentral gyrus	0.26	0.66	0.31
(6) Right insula	0.24	0.72	0.13
(7) Right middle frontal gyrus	0.14	0.21	0.96
(8) Left middle frontal gyrus	0.14	0.20	0.71
(9) Left superior temporal sulcus	0.26	0.82	0.20

Table 2. The factor loadings for each of the nine selected ROIs.

and cognition (Ray & Zald, 2012). Regarding the negatively correlated regions, within the first subsystem, the precuneus and postcentral gyrus (Cavanna & Trimble, 2006) have been associated with selective attention (Alho et al., 2006; Degerman, Rinne, Salmi, Salonen, & Alho, 2006) and the detection of agency in person attribution (Mar, Kelley, Heatherton, & Macrae, 2007), the right insula has been associated with negative emotions (Damasio et al., 2000; Fan et al., 2011; Suslow et al., 2009), and the left superior temporal sulcus has been associated with emotional face appraisals (Grosbras & Paus, 2006). The second subsystem, the bilateral middle frontal gyri, is also part of the default network, which is a system for internal mental activity that works in competition with external sensory processing (Buckner, Andrews-Hanna, Schacter, 2008; Fox et al., 2005); therefore, greater attention to external stimuli results in less activity in the default network. Deactivations of the middle frontal areas have also been reported when subjects showed decreased self-awareness in highly engaging perceptual tasks (Goldberg, Harel, & Malach, 2006) and may be associated with task-engagement/absorption in the FFD. Given the intricate inner workings of perception and emotion, and the inherent problems that are associated with reverse inference (Ramsey et al., 2010), currently we can only speculate on the functional roles of these systems. The individual differences among the 14 subjects (as shown in Figure 8a) may concur with the two-system hypothesis, i.e., the segregation of perceptual and emotion/engagement systems. The higher correlations of positively rating-related ROIs ($r = 0.73$) relative to the negatively rating-correlated ROIs ($r = 0.5$) may reflect the notion that, although participants perceptually process FFD stimuli quite similarly, they differ in their subjective appraisals of grotesqueness, bizarreness, and the variable temporal engagement of the illusion.

In the literature, there is a related phenomenon called the face distortion after-effect (FDAE, Webster & MacLin, 1999). The FDAE occurs when participants

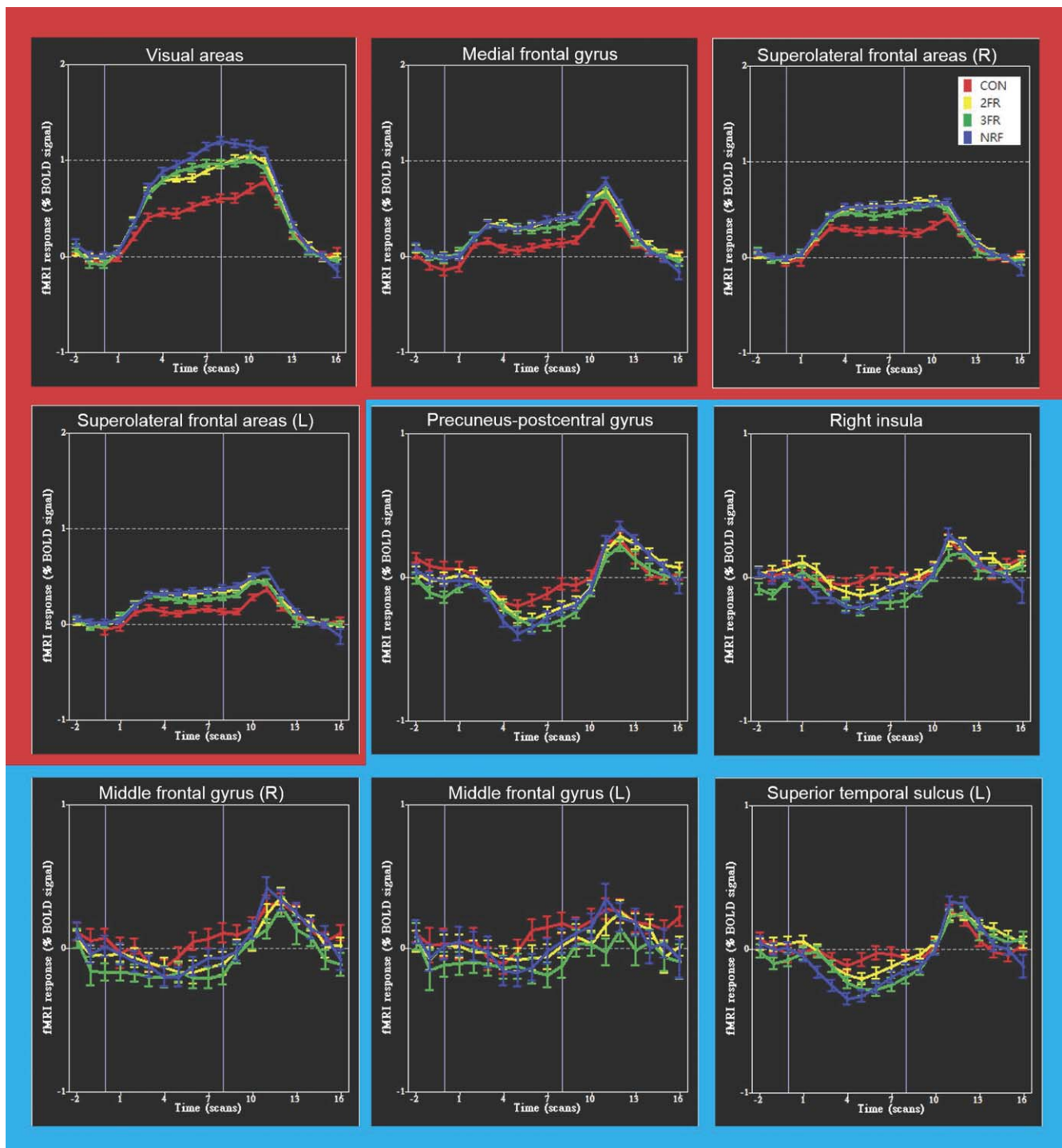


Figure 7. The average time courses of all participants in the nine identified rating-correlated ROIs. The red background illustrates positive rating-correlated regions, while the blue background illustrates negative rating-correlated regions.

spend several seconds to several minutes staring at an artificially distorted face, followed by viewing a normal face, making the normal face appear “distorted” in the opposite direction, such as an elongated chin becoming shortened. Both human psychophysics (Leopold, Rhodes, Muller, & Jeffery, 2005) and monkey neurophysiology (Leopold, Bondar, & Giese, 2006) have

suggested that long-term exposure to a particular stimulus decreases the responses of feature-selective visual neurons. Using fMRI, researchers have also observed decreased responses in both early visual and face-selective temporal areas that are involved in the FDAE (Kovacs, Cziraki, Vidnyanszky, Schweinberger, & Greenlee, 2008; Kovacs, Iffland, Vidnyanszky, &

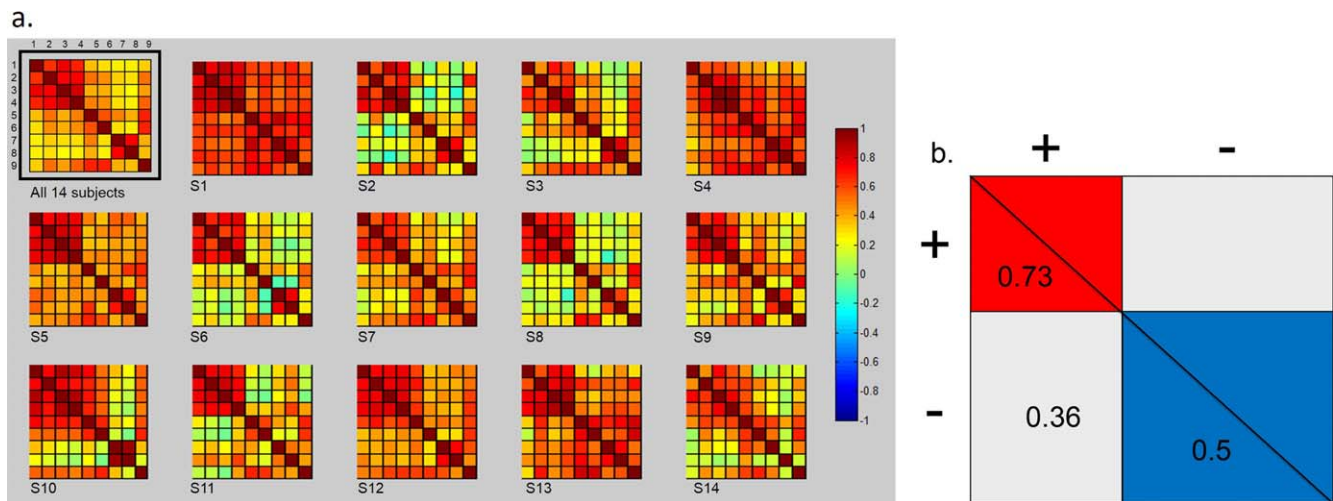


Figure 8. (a) Graphical representation of the correlation matrices for the following ROIs: (1) visual-parietal areas, (2) medial frontal gyrus, (3) right superolateral frontal areas, (4) left superolateral frontal areas, (5) precuneus-postcentral gyrus, (6) right insula, (7) right middle frontal gyrus, (8) left middle frontal sulcus, and (9) left superior temporal sulcus. (b) An illustration showing the overall grouping of the average correlation matrix (top left of Figure 8a). Red regions represent the correlations among positive rating-correlated ROIs ($r = 0.73$), blue regions represent the correlation among negative rating-correlated ROIs ($r = 0.5$). In addition, both intercorrelations are significantly higher than the correlations of opposite directional ROIs, $r = 0.36$, and $t(19) = 10.3$, $p < 0.001$, and $t(28) = 3.36$, $p = 0.002$, respectively.

Greenlee, 2012; Nagy, Zimmer, Greenlee, & Kovacs, 2012; Zimmer & Kovacs, 2011). Similarly, the current study found that retinotopy-defined visual areas and face-selective areas (e.g., rFFA, rOFA, and rSTS) are also involved in the FFD.

Lastly, here we have to mention a possible shortcoming of the present study: The perceived FFD strength as rated by participants confounds with the neuronal adaptations associated with the number of faces per sequence. One can argue that the different amounts of activation observed in the current study are attributed to different amounts of fMRI adaptation (fMRIa; Grill-Spector, Henson, & Martin, 2006), defined as the reduction in the BOLD signal after repeated exposure to the same stimulus. It has been demonstrated that the BOLD response decreases in proportion to the repeated stimuli frequency (Grill-Spector, Edelman, Kushnir, Itzhak, & Malach, 1999; Konen & Kastner, 2008; Rhodes, Michie, Hughes, & Byatt, 2009). fMRIa has been used to study the responses of brain regions to invariant properties, such as viewpoints, expressions, and illumination (Grill-Spector & Malach, 2001; Winston, Henson, Fine-Goulden, & Dolan, 2004), where areas representing invariant properties show reduced signal after repetition. One might argue that our findings are merely that of fMRIa. Although adaptation likely plays a role in the FFD, we suggest four points worth considering. First, both blocked (Konen & Kastner, 2008) and event-related (Fang, Murray, & He, 2007; Fang, Murray, Kersten, & He, 2005) fMRIa studies have shown that short-term adaptation is not easily found in

the early visual areas, but only in intermediate and high-level areas. Our display time for each individual stimulus in the FFD demonstration was 250 ms, which should cause little or no adaptation effect in the early visual areas. Hence the differential activity observed is probably attributed to top-down feedback processes from higher level areas. Second, fMRIa studies were mostly achieved through central viewing; in contrast, the FFD is exclusively generated in the peripheral vision. Kovacs et al. (2012) found minimal or no adaptation effect in peripheral representations within the early visual areas, suggesting that the parafoveal/peripheral areas are less responsive to changes in face number. Third, our voxelwise correlation also revealed several nonvisual areas (including the frontal areas, insula, etc.) that were positively and negatively correlated with ratings, rendering the number of faces account incapable of fully explaining the pattern of our results. Fourth, in illusion aftereffects such as the FDAE, greater adaptation leads to stronger aftereffects (Kovacs et al., 2008; Rhodes, Jeffery, Clifford, & Leopold, 2007). In contrast, the FFD paradigm found stronger illusion strengths in the less adapted conditions, with associative higher BOLD signals. In other words, in the FFD, *decreased* BOLD adaptation is associated with a *stronger* FFD illusion. Despite the evidence that is incompatible with the adaptation account, we still acknowledge that a future study may consider including another category of objects (such as cars or houses) that does not cause the FFD as a control category. Such an experiment would help tease apart the effects caused by the FFD and different

adaptations caused by the varying number of stimuli per sequence. However, such a proposal will still need to control for other factors when making comparisons with faces, such as eye alignment, shape similarity, and significance/salience, just to name a few.

Conclusions

In conclusion, our findings provide the first look into the brain networks that are responsible for the FFD. They consist of the early visual areas, face-selective areas, and two additional groups including nonvisual regions: one for perceptual processing, and two other subsystems for aspects of emotion and/or engagement.

Keywords: flashed face distortion, fMRI, illusion, exploratory factor analysis, retinotopic mapping.

Acknowledgments

The authors would like to thank the Ministry of Science and Technology (MOST) in Taiwan for their financial support (Contract Nos. NSC102-2815-C-006-016-H to TW and NSC102-2420-H-006-008 to CCK). This research was supported in part by the “Top Notch” Project of NCKU (D103-36A06) by the Taiwan Ministry of Education. We would also like to thank the consultation and instrument availability provided by the NCKU MRI Center, supported by the MOST.

Commercial relationships: none.

Corresponding author: Chun-Chia Kung.

Email: chunkung@mail.ncku.edu.tw.

Address: Department of Psychology, National Cheng Kung University, Tainan City, Taiwan.

References

- Alho, K., Vorobyev, V. A., Medvedev, S. V., Pakhomov, S. V., Starchenko, M. G., Tervaniemi, M., & Naatanen, R. (2006). Selective attention to human voice enhances brain activity bilaterally in the superior temporal sulcus. *Brain Research, 1075*(1), 142–150, doi:10.1016/j.brainres.2005.11.103.
- Andrews, T. J., Schluppeck, D., Homfray, D., Matthews, P., & Blakemore, C. (2002). Activity in the fusiform gyrus predicts conscious perception of Rubin’s vase-face illusion. *Neuroimage, 17*(2), 890–901.
- Baumann, S., Koeneke, S., Schmidt, C. F., Meyer, M., Lutz, K., & Jancke, L. (2007). A network for audio-motor coordination in skilled pianists and non-musicians. *Brain Research, 1161*, 65–78, doi:10.1016/j.brainres.2007.05.045.
- Brainard, D. H. (1997). The Psychophysics Toolbox. *Spatial Vision, 10*(4), 433–436.
- Buckner, R. L., Andrews-Hanna, J. R., & Schacter, D. L. (2008). The brain’s default network: anatomy, function, and relevance to disease. *Annals of the New York Academy of Sciences, 1124*, 1–38, doi:10.1196/annals.1440.011.
- Cavanna, A. E., & Trimble, M. R. (2006). The precuneus: A review of its functional anatomy and behavioural correlates. *Brain, 129*(Pt 3), 564–583, doi:10.1093/brain/awl004.
- Corina, D., Chiu, Y. S., Knapp, H., Greenwald, R., San Jose-Robertson, L., & Braun, A. (2007). Neural correlates of human action observation in hearing and deaf subjects. *Brain Research, 1152*, 111–129, doi:10.1016/j.brainres.2007.03.054.
- Damasio, A. R., Grabowski, T. J., Bechara, A., Damasio, H., Ponto, L. L., Parvizi, J., & Hichwa, R. D. (2000). Subcortical and cortical brain activity during the feeling of self-generated emotions. *Nature Neuroscience, 3*(10), 1049–1056, doi:10.1038/79871.
- de Borst, A. W., Sack, A. T., Jansma, B. M., Esposito, F., de Martino, F., Valente, G., . . . Formisano, E. (2012). Integration of “what” and “where” in frontal cortex during visual imagery of scenes. *Neuroimage, 60*(1), 47–58, doi:10.1016/j.neuroimage.2011.12.005.
- Degerman, A., Rinne, T., Salmi, J., Salonen, O., & Alho, K. (2006). Selective attention to sound location or pitch studied with fMRI. *Brain Research, 1077*(1), 123–134, doi:10.1016/j.brainres.2006.01.025.
- Eysel, U. T. (2003). Illusions and perceived images in the primate brain. *Science, 302*(5646), 789–791, doi:10.1126/science.1091065.
- Fan, J., Gu, X., Liu, X., Guise, K. G., Park, Y., Martin, L., . . . Hof, P. R. (2011). Involvement of the anterior cingulate and frontoinsula cortices in rapid processing of salient facial emotional information. *Neuroimage, 54*(3), 2539–2546, doi:10.1016/j.neuroimage.2010.10.007.
- Fang, F., Murray, S. O., & He, S. (2007). Duration-dependent fMRI adaptation and distributed viewer-centered face representation in human visual cortex. *Cerebral Cortex, 17*(6), 1402–1411, doi:10.1093/cercor/bhl053.
- Fang, F., Murray, S. O., Kersten, D., & He, S. (2005). Orientation-tuned fMRI adaptation in human

- visual cortex. *Journal of Neurophysiology*, 94(6), 4188–4195, doi:10.1152/jn.00378.2005.
- Fox, M. D., Snyder, A. Z., Vincent, J. L., Corbetta, M., Van Essen, D. C. & Raichle, M. E. (2005). The human brain is intrinsically organized into dynamic, anticorrelated functional networks. *Proceedings of the National Academy of Sciences*, 102(27), 9673–9678, doi:10.1073/pnas.0504136102.
- Goldberg, I. I., Harel, M., & Malach, R. (2006). When the brain loses its self: Prefrontal inactivation during sensorimotor processing. *Neuron*, 50(2), 329–339, doi:10.1016/j.neuron.2006.03.015.
- Gregory, R. L. (1968). Perceptual illusions and brain models. *Proceedings of the Royal Society of London B: Biological Science*, 171(1024), 279–296.
- Grill-Spector, K., Edelman, S., Kushnir, T., Itzhak, Y., & Malach, R. (1999). Differential processing of objects under various viewing conditions in the human lateral occipital complex. *Investigative Ophthalmology & Visual Science*, 40(4), S399.
- Grill-Spector, K., Henson, R., & Martin, A. (2006). Repetition and the brain: Neural models of stimulus-specific effects. *Trends in Cognitive Sciences*, 10(1), 14–23, doi:10.1016/j.tics.2005.11.006.
- Grill-Spector, K., & Malach, R. (2001). fMR-adaptation: A tool for studying the functional properties of human cortical neurons. *Acta Psychologica*, 107(1–3), 293–321, doi:10.1016/S0001-6918(01)00019-1.
- Grosbras, M. H., & Paus, T. (2006). Brain networks involved in viewing angry hands or faces. *Cerebral Cortex*, 16(8), 1087–1096, doi:10.1093/cercor/bhj050.
- Habeck, C., Rakitin, B. C., Moeller, J., Scarmeas, N., Zarahn, E., Brown, T., & Stern, Y. (2005). An event-related fMRI study of the neural networks underlying the encoding, maintenance, and retrieval phase in a delayed-match-to-sample task. *Brain Research: Cognitive Brain Research*, 23(2–3), 207–220, doi:10.1016/j.cogbrainres.2004.10.010.
- Hasson, U., Hendler, T., Ben Bashat, D., & Malach, R. (2001). Vase or face? A neural correlate of shape-selective grouping processes in the human brain. *Journal of Cognitive Neuroscience*, 13(6), 744–753, doi:10.1162/08989290152541412.
- Haxby, J. V., Hoffman, E. A., & Gobbini, M. I. (2000). The distributed human neural system for face perception. *Trends in Cognitive Sciences*, 4(6), 223–233, doi:10.1016/S1364-6613(00)01482-0.
- Konen, C. S., & Kastner, S. (2008). Two hierarchically organized neural systems for object information in human visual cortex. *Nature Neuroscience*, 11(2), 224–231, doi:10.1038/Nn2036.
- Koshino, H., Carpenter, P. A., Minshew, N. J., Cherkassky, V. L., Keller, T. A., & Just, M. A. (2005). Functional connectivity in an fMRI working memory task in high-functioning autism. *Neuroimage*, 24(3), 810–821, doi:10.1016/j.neuroimage.2004.09.028.
- Kovacs, G., Cziraki, C., Vidnyanszky, Z., Schweinberger, S. R., & Greenlee, M. W. (2008). Position-specific and position-invariant face aftereffects reflect the adaptation of different cortical areas. *Neuroimage*, 43(1), 156–164, doi:10.1016/j.neuroimage.2008.06.042.
- Kovacs, G., Iffland, L., Vidnyanszky, Z., & Greenlee, M. W. (2012). Stimulus repetition probability effects on repetition suppression are position invariant for faces. *Neuroimage*, 60(4), 2128–2135, doi:10.1016/J.Neuroimage.2012.02.038.
- Kuriki, I., Ashida, H., Murakami, I., & Kitaoka, A. (2008). Functional brain imaging of the rotating snakes illusion by fMRI. *Journal of Vision*, 8(10): 16, 1–10, <http://www.journalofvision.org/content/8/10/16>, doi:10.1167/8.10.16. [PubMed] [Article]
- Leopold, D. A., Bondar, I. V., & Giese, M. A. (2006). Norm-based face encoding by single neurons in the monkey inferotemporal cortex. *Nature*, 442(7102), 572–575, doi:nature04951 [pii] 10.1038/nature04951.
- Leopold, D. A., Rhodes, G., Muller, K. M., & Jeffery, L. (2005). The dynamics of visual adaptation to faces. *Proceedings of the Royal Society B: Biological Sciences*, 272(1566), 897–904, doi:10.1098/Rspb.2004.3022.
- Mar, R. A., Kelley, W. M., Heatherton, T. F., & Macrae, C. N. (2007). Detecting agency from the biological motion of veridical vs animated agents. *Social Cognitive and Affective Neuroscience*, 2(3), 199–205, doi:10.1093/scan/nsm011.
- Mashal, N., Faust, M., & Hendler, T. (2005). The role of the right hemisphere in processing nonsalient metaphorical meanings: Application of principal components analysis to fMRI data. *Neuropsychologia*, 43(14), 2084–2100, doi 10.1016/J.Neuropsychologia.2005.03.019.
- Mclaughlin, T., Steinberg, B., Christensen, B., Law, I., Parving, A., & Friberg, L. (1992). Potential language and attentional networks revealed through factor-analysis of rCBF data measured with SPECT. *Journal of Cerebral Blood Flow & Metabolism*, 12(4), 535–545.
- Morita, T., Kochiyama, T., Okada, T., Yonekura, Y., Matsumura, M., & Sadato, N. (2004). The neural substrates of conscious color perception demon-

- strated using fMRI. *Neuroimage*, 21(4), 1665–1673, doi:10.1016/j.neuroimage.2003.12.019.
- Nagy, K., Zimmer, M., Greenlee, M. W., & Kovacs, G. (2012). Neural correlates of after-effects caused by adaptation to multiple face displays. *Experimental Brain Research*, 220(3–4), 261–275, doi:10.1007/s00221-012-3135-3.
- Peterson, B. S., Skudlarski, P., Gatenby, J. C., Zhang, H. P., Anderson, A. W., & Gore, J. C. (1999). An fMRI study of Stroop word-color interference: Evidence for cingulate subregions subserving multiple distributed attentional systems. *Biological Psychiatry*, 45(10), 1237–1258, doi:10.1016/S0006-3223(99)00056-6.
- Ramsey, J. D., Hanson, S. J., Hanson, C., Halchenko, Y. O., Poldrack, R. A., & Glymour, C. (2010). Six problems for causal inference from fMRI. *Neuroimage*, 49(2), 1545–1558, doi:10.1016/j.neuroimage.2009.08.065.
- Ray, R. D., & Zald, D. H. (2012). Anatomical insights into the interaction of emotion and cognition in the prefrontal cortex. *Neuroscience and Behavioral Reviews*, 36(1), 479–501, doi:10.1016/j.neubiorev.2011.08.005.
- Rhodes, G., Jeffery, L., Clifford, C. W. G., & Leopold, D. A. (2007). The timecourse of higher-level face aftereffects. *Vision Research*, 47(17), 2291–2296, doi:10.1016/j.visres.2007.05.012.
- Rhodes, G., Michie, P. T., Hughes, M. E., & Byatt, G. (2009). The fusiform face area and occipital face area show sensitivity to spatial relations in faces. *European Journal of Neuroscience*, 30(4), 721–733, doi:10.1111/J.1460-9568.2009.06861.X.
- Roth, J. K., Johnson, M. K., Raye, C. L., & Constable, R. T. (2009). Similar and dissociable mechanisms for attention to internal versus external information. *Neuroimage*, 48(3), 601–608, doi:10.1016/j.neuroimage.2009.07.002.
- Suslow, T., Kugel, H., Rauch, A. V., Dannlowski, U., Bauer, J., & Konrad, C.,...Ohrmann, P. (2009). Attachment avoidance modulates neural response to masked facial emotion. *Human Brain Mapping*, 30(11), 3553–3562, doi:10.1002/hbm.20778.
- Talairach, J., & Tournoux, P. (1998). 3-dimensional proportional system: an approach to cerebral imaging. *Co-planar stereotaxic atlas of the human brain*. New York: Thieme.
- Tangen, J. M., Murphy, S. C., & Thompson, M. B. (2011). Flashed face distortion effect: Grotesque faces from relative spaces. *Perception*, 40(5), 628–630.
- Wandell, B. A., & Smirnakis, S. M. (2009). Plasticity and stability of visual field maps in adult primary visual cortex. *Nature Reviews Neuroscience*, 10(12), 873–884, doi:10.1038/nrn2741.
- Wang, K., Liang, M., Wang, L., Tian, L., Zhang, X., Li, K., & Jiang, T. (2007). Altered functional connectivity in early Alzheimer's disease: A resting-state fMRI study. *Human Brain Mapping*, 28(10), 967–978, doi:10.1002/hbm.20324.
- Warnking, J., Dojat, M., Guerin-Dugue, A., Delon-Martin, C., Olympieff, S., & Richard, N.,...Segebarth, C. (2002). FMRI retinotopic mapping—Step by step. *Neuroimage*, 17(4), 1665–1683, doi:10.1006/Nimg.2002.1304.
- Webster, M. A., & MacLin, O. H. (1999). Figural aftereffects in the perception of faces. *Psychonomic Bulletin Review*, 6(4), 647–653.
- Wen, T., Li, W. L., & Kung, C. C. (1999). On factors affecting the flashed face distortion effect. Poster presented at the 50th Annual Convention of the Taiwanese Psychological Association. Poster presented at the 50th Annual Convention of the Taiwanese Psychological Association, Asia University, Taiwan, 15–16 October, 2011.
- Winston, J. S., Henson, R. N. A., Fine-Goulden, M. R., & Dolan, R. J. (2004). fMRI-adaptation reveals dissociable neural representations of identity and expression in face perception. *Journal of Neurophysiology*, 92(3), 1830–1839, doi:10.1152/jn.00155.2004.
- Woolgar, A., Thompson, R., Bor, D., & Duncan, J. (2011). Multi-voxel coding of stimuli, rules, and responses in human frontoparietal cortex. *Neuroimage*, 56(2), 744–752, doi:10.1016/j.neuroimage.2010.04.035.
- Zimmer, M., & Kovacs, G. (2011). Position specificity of adaptation-related face aftereffects. *Philosophical Transactions of the Royal Society of London B: Biological Sciences*, 366(1564), 586–595, doi:10.1098/rstb.2010.0265.